INTERNATIONAL ATOMIC ENERGY AGENCY
UNITED NATIONS EDUCATIONAL, SCIENTIFIC AND CULTURAL ORGANIZATION

INTERNATIONAL CENTRE FOR THEORETICAL PHYSICS
34100 TRIESTE (ITALY) - P.O.B. 586 - MIRAMARE - STRADA COSTIERA 11 - TELEPHONE: 2240-1
CABLE: CENTRATOM - TELEX 460392-1

H4.SMR/204 - 40

WINTER COLLEGE ON

ATOMIC AND MOLECULAR PHYSICS

(9 March - 3 April 1987)

SURFACE DIAGNOSTICS

C. FLYTZANIS

Laboratoire d'Optique Quantique
Ecole Polytechnique
91128 Palaiseau
France

Surfaces play a very important role in many areas of both fundamental and technological interest. In order to understand their properties and exploit the applications can be made out of them physicists & chemists have developped different surface diagnostic techniques.

These techniques are varied depending on the problem that one is addressing. In these lectures I will concentrate myself on two

- Surface Enhanced Nonlinear Optical Techniques
- Molecular beam Scattering on Surfaces and their diagnostic with lasers.

The both address problems related to molecule/surface interaction but their objectives are different. Thus in the

first technique one uses particular aspects of the adsorbed molecule/surface complex to enhance the optical properties of the adsorbed molecule and extract information about molecular monolayer on surfaces. In the second technique one prepares the molecules before the collision with the surface in a given quantum state and interrogates them after the collision to find at what state the are.

In the first technique massless particles (photons) are used and one studies induced optical effects, mainly nonlinear; the surfaces do not need to be in vaccuum. In the second case one uses massive particles (molecules) with internal degrees of freedom (rotation, vibration) and

is interested in the energy exchange & transfer between molecule & surface and ~~vice versa~~ (energy accomodation); here one needs high vacuum better than 10^{-8}–10^{-9} torr and this leads to quite complicated experimental set ups.

Of the five lectures, three will be devoted to the first topic & the other two to the second topic. To be more specific

1. General introduction to surface enhanced nonlinear optical effect. Raman Scattering
2. Second harmonic generation from surfaces
3. Optical phase conjugation from small metallic particles. Surface enhanced Optical Kerr effect.
4. Experimental investigations of Laser diagnostic of molecular beam scattering on surfaces
5. Dynamical Processes in molecular beam Scattering at Surfaces.

Physical Origin of Surface Enhancement.

The main mechanisms are

- molecule surface contact interaction (<0.1 Å) it only concerns the first molecular layer
- image field effect (selfaction) ~2-3 Å
- local field effect due to roughness it extends to several tens of Å.

From simple order of magnitude argument and experimental evidence one finds that the local field effect is the dominant mechanism that count for most of the enhancement.

In the case of Raman scattering the observed enhancement can be as high as 10^7 and this can be accounted for with the local field factor from rough surfaces. The other two mechanisms which are of very short range can give some additional enhancement even in clean flat surfaces.

the surface enhancement can be calculated easily from the following model

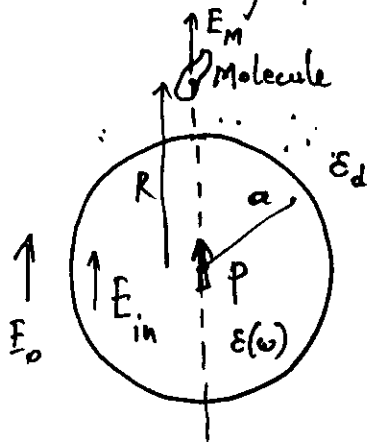

$$E_{in} = \frac{3\epsilon_d}{\epsilon(\omega)+2\epsilon_d} E_0$$

$$p = \frac{\epsilon-\epsilon_d}{3} a^3 E_{in}$$

$$E_M = E_0 + 2\frac{a^3}{R^3}\frac{\epsilon-\epsilon_d}{\epsilon+2\epsilon_d} E_0$$

one sees that E_M is enhanced when

$$\varepsilon'_m(\omega_s) = -2\epsilon_d \qquad (\epsilon_m = \varepsilon'_m + i\varepsilon''_m)$$

which occurs for a frequency ω_s the surface plasmon frequency.

One can also calculate the field for an ellipsoid and the condition then is

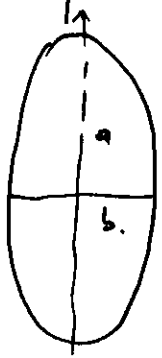

$$\epsilon'(\omega_s) = \epsilon_d\left(1-\frac{1}{A}\right)$$

$$A = (\eta_0^2-1)\left(\frac{1}{2}\eta_0 \ln\frac{\eta_0+1}{\eta_0-1} - 1\right).$$

$$\eta_0 = \frac{a}{\sqrt{a^2-b^2}}$$

If we define

$$f(\omega) = \frac{E_m}{E_0}$$

Then one has

* Raman Cross Section

$$\frac{d\sigma}{d\Omega} = \frac{\hbar}{2\rho v_1}\frac{\omega_L \omega_S^3}{c^4} f(\omega_L)^2 f(\omega_S)^2 \left(\frac{\partial\alpha}{\partial q}\right)^2$$

* Second harmonic

$$P^{(2)}_{2\omega} = \chi^{(2)}(\omega,\omega) E_\omega E_\omega$$

$$I_{2\omega} = \frac{32\pi^3\omega^2}{c^3}\sec^2\vartheta \left|\hat{e}_2 \tilde{\chi}_s \hat{e}_1 \hat{e}_1\right| I_\omega^2$$

$$\chi^{(2)} = N f_{2\omega} f_\omega^2 \alpha^{(2)}(\omega,\omega)$$

* Optical Kerr effect: (metal colloids).

$$\tilde{n}^2 = (n_0 + n_2 I)^2 = \varepsilon_0 + \delta\tilde{\epsilon}$$

$$\delta\tilde{\epsilon} = 12\pi p f_\omega^4 \chi^{(3)}_m E_0^2. \qquad p \text{ particle concentration}$$

Main References.

M. Moskovits. Rev. Mod. Phys. 57, 783 (85).

D. Ricard, in Nonlinear Optics: Devices & Materials, Springer Verlag (Eds Flytzanis & Oudar). 1986.

D Ricard P. Roussignol, C. Flytzanis. Opt. Lett. 10, 511 (85).

The first reference gives a rather general overview of surface enhanced phenomena in general has detailed references and compares different models.

The second concentrate on second harmonic on surfaces

The third discusses the optical Kerr effect in colloid particles.

From the above reference one can find most of the information one needs for further reading.

Through this simple model one can then proceed to more sophisticated considerations.

The first Brill. Raman Scattering effect was seen by Fleischmann, Hendra, McQuillan (Chem. Phys. Lett. 26, 163 (1974)) and more formly by Jeanmaire van Duyne (J. Electroanal) Chem. 84, 1(77).

The second harmonic generation has been particularly studied in Berkeley by Shen et al

The surface enhanced optical Kerr effect has been firstst proposed & observed by Ricard et al (Opt. Lett. 10, 511 (85).

There is continuous interest in this area in particular in nonlinear optics second harmonic & frequency mixing (IR + optical) is becoming a reliable tool for study of surface structure with ultrashort pulses (femtoseconds) to avoid thermal effects.

Proceedings of Materials Research Society Meeting
Dec. 2-7/85 Boston

DYNAMICS OF ELEMENTARY PROCESSES AT SURFACES: NITRIC OXIDE SCATTERED FROM A GRAPHITE SURFACE

H. VACH, J. HÄGER, B. SIMON, C. FLYTZANIS*, AND H. WALTHER
Max-Planck-Institut für Quantenoptik, D8046 Garching and
Sektion Physik der Universität München, Fed. Rep. of Germany

ABSTRACT

Molecular beam scattering from solid surfaces has long been recognized as a powerful means for investigation of gas-surface reaction dynamics. With the help of the recently developed laser-induced fluorescence and ionization techniques for state-selective detection, one can now measure the angular and velocity distributions of the scattered molecules together with their internal energy distributions. Such measurements fully describe the average energy and momentum exchanges between molecules and surfaces and give thus full information on the dynamics of the interaction. Recently, also the scattering of vibrationally excited NO molecules was investigated. The paper gives a review of new experiments with emphasis on the investigation of the scattering of NO molecules from a pyrographite surface. A simple model using transport properties of the solid is presented which accounts surprisingly well for the observed features.

INTRODUCTION

In recent years a large amount of detailed information has been obtained on the interaction of gases with clean single-crystal surfaces. The knowledge on binding sites of adsorbed molecules and their vibrational motion has been provided by infrared absorption [1] and electron energy loss spectroscopy [2]. Binding energies and residence times can be investigated by temperature dependent desorption [3] and modulated molecular beam techniques [4]. Furthermore, angular and velocity distributions of scattered particles provide information on the corrugation and the repulsive part of the interaction potential responsible for the translational energy exchange [5].

Further progress was made when molecular beam scattering from surfaces was combined with subsequent analysis by laser techniques leading to the distribution of the internal degrees of freedom of the scattered molecules as well as their angle and state resolved velocity distributions [6 - 14]. These laser measurements provide new and surprising results on the scattering process, not available by conventional methods. It could be observed that both trapping/desorption and inelastic scattering processes show similar behaviour for the rotational state distribution: the molecules were fully accommodated to the surface at low surface temperatures, but not at higher ones. The observed results do not depend on the kinetic energy of the incoming particles for the case of adsorption/desorption and show a small change in the case of inelastic scattering. This is the case as long as the velocities of the incoming particles are in the range of thermal energies. Higher translational energies (> 0.4 eV) lead to rotational rainbows and to a polarization of the scattered particles [7].

The laser investigation of the vibrational motion of the particles shows excitation of the molecules during the scattering process that is dependent on both the incoming translational energy and the surface temperature [7e]. In general, it has been observed that there is only a very inefficient vibrational energy transfer to the scattering surface, i.e. vibrational accommodation coefficients are small. This was predicted theoretically [15] and observed experimentally [10b].

The study of NO molecules desorbing from a Pt(111) surface showed accommodation of the velocity distributions to the surface temperature for intermediate temperature ranges [9c]. This result could be expected according to the mainly isotropic angular distributions which were found experimentally [6c, 9c]. In the case of the inelastic NO/graphite system, however, a more complicated velocity distribution was measured [6d]. At low surface temperatures two different scattering channels exist: one corresponding to quasi-specularly reflected molecules with a velocity slightly smaller than that of the incoming beam, while the other one represents a diffusively scattered part with particles with a much smaller velocity. The peak velocity of the quasi-specularly scattered molecules increases with increasing surface temperature, increasing incidence and decreasing scattering angle. This effect can be so substantial that some of the scattered molecules show a velocity larger than that of the incoming ones, especially for high surface temperatures, large incidence and small scattering angles.

In the following the results of our investigations into the scattering of NO molecules from a graphite surface will be discussed in more detail.

* Permanent address: Laboratoire d'Optique Quantique, Ecole Polytechnique, 91128 - Palaiseau, Cedex, France

EXPERIMENTAL

An ultrahigh vacuum (UHV) chamber with a pulsed or optionally continuous molecular beam was developed for measuring the angular, rotational, vibrational and velocity distributions of surface scattered NO molecules. The details of this set-up have already been described [6]. The NO molecules of an (optionally seeded) supersonic molecular beam are scattered from a cleaved pyrographite surface in the centre of an UHV chamber (background gas pressure 10^{-10} mbar). The molecular beam is crossed by the frequency doubled radiation of a tunable excimer pumped dye laser (226 nm). The laser beam can be positioned in such a way that it probes either the incoming or the scattered molecules. The NO molecules are excited electronically in a one-photon process or ionized by resonantly enhanced two-photon absorption. The fluorescence intensity or the number of ionized molecules is recorded as a function of the laser wavelength. The population density of the rotational and vibrational levels can be deduced from the line intensities of the resulting spectra. In addition, information on the angle and state resolved velocity distributions of the scattered molecules can be obtained [6d]. For this purpose a cylindrical cage of metal wire mesh is set in front of the sample, with the focused laser beam propagating along the cage axis. Scattered molecules passing through the centre of the cage are ionized, starting from a specific rotational-vibrational state, by a resonantly enhanced two-photon transition. The ions produced have the same velocity as the parent molecules. Changing the position of the surface relative to the cage leads to a detection of molecules with different scattering angles.

For the investigation of the scattering behaviour of vibrationally excited molecules part of the incoming particles are excited into the first vibrational state by a CO-laser pumped Spin-Flip Raman laser (SFL), tuned to the R(1/2) NO line. The SFL beam is focused into a multireflection cell (White cell) properly adjusted for efficient excitation of the incoming molecular beam (Fig. 1).

The degree of vibrational excitation of the incoming NO molecules by the SFL is limited owing to both the small absorption linewidth of the incoming molecular beam and the relatively high number of populated rotational states. We estimate, however, that about 2 per cent of the incoming particles are excited into the $v = 1$ ($J = 3/2$) state. In order to probe the vibrational excitation of the scattered molecules, the frequency-doubled dye laser was tuned over the $^2\Pi$ ($v = 1$) $\rightarrow$ $^2\Sigma$($v = o$) transition (around 236 nm), leading to fluorescence or ionization spectra and, consequently, to both rotational ard angular distributions of vibrationally excited molecules.

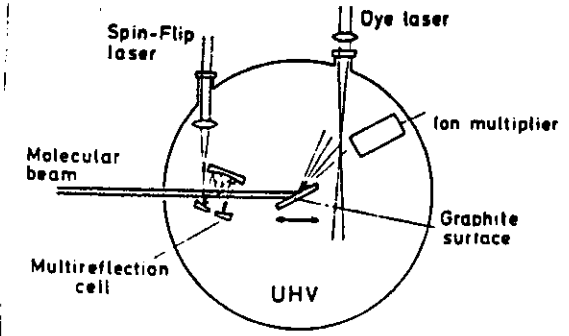

Fig. 1: Schematic set-up for the investigation of the scattering of vibrationally excited NO molecules.

The NO molecules were scattered from the surface of a cleaved pyrolytic graphite crystal or from a carbon-covered Pt(111) surface. The graphite crystal consisted of microcrystals with highly oriented basal planes and a mosaic spread of 0.4° ± 0.1° (Union Carbide, grade ZYA).

RESULTS

The adiabatic expansion of the NO molecular beam in the nozzle causes an increase of the average velocity in the beam direction and, simultaneously, a strong reduction of the rotational temperature and the velocity spread. The unseeded molecules in our supersonic beam had an average velocity of ~ 750 m/s, a velocity spread (FWHM) of ~ 140 m/s and a rotational population distribution corresponding to about 35 K [6]. The beam impinged on the surface at a selectable incidence angle between 30° and 70°. The NO/graphite system has a very low interaction potential depth (0.1 eV), leading to a very short residence time of the molecules on the surface. This time is short compared with the duration of the molecular beam pulses (~ 5 ms FWHM).

The angular distributions of NO molecules scattered from the graphite surface clearly indicate the weakly inelastic character of the interaction [6b]. At low T_s, the distributions are generally composed of a quasi-specular scattering or lobular part peaked at a scattering angle θ_s significantly less than the specular reflection angle and a diffusive scattering or cosine distribution part. With increasing surface temperature, the diffusive part decreases relative to the specular part together with a shift of the specular lobe to lower scattering angles. This behaviour results from a weakly inelastic scattering process with an increasing trapping/desorption contribution

for decreasing temperatures. The change of the angle of the specular lobe is correlated with the behaviour of the velocity distributions of the scattered NO molecules, as will be discussed later.

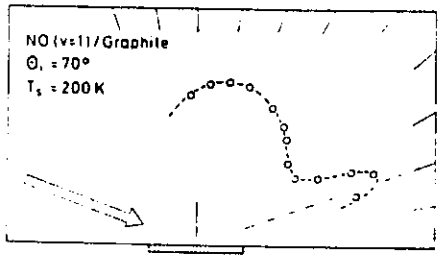

Fig. 2: Angular distribution of vibrationally excited NO molecules scattered from a 200 K graphite surface.

The vibrationally excited molecules show a similar behaviour. For the measurements shown in Fig. 2, the incoming molecules had a velocity of 1400 m/s (NO seeded in He), an incidence angle of 70°, and were excited to the v = 1 (J = 3/2) state. The laser probed only NO molecules which were scattered from the 200 K graphite surface into the v = 1 (J = 11/2) state, that means molecules with preserved vibrational and changed rotational state. The vibrationally excited molecules exhibit a specular scattering lobe and a diffusive part very similar to the results obtained for the molecules in the vibrational ground state [6b]. Within the given experimental accuracy the angular distributions of the scattered molecules seem to be independent of the rotational and of, in addition, the vibrational state.

The rotational distributions of both the vibrational ground state and the first vibrational state were derived from the spectra of the $^2\Pi$ (v = 0) → $^2\Sigma$ (v = 0) transition (~ 226 nm) and the $^2\Pi$ (v = 1) → $^2\Sigma$ (v = 0) transition (~ 236 nm), respectively. In both cases, the rotational state population could be fitted approximately to Boltzmann distributions with a characteristic rotational temperature T_{rot}. For the ground state measurements, it was found that the population distribution in the electronic states $^2\Pi_{1/2}$ and $^2\Pi_{3/2}$ could be described by the same T_{rot}. Even the overall population ratio $N(^2\Pi_{1/2})$: $N(^2\Pi_{3/2})$ is given roughly by $\exp(-\Delta E/kT_{rot})$, where ΔE is the fine-structure splitting.

The dependence of T_{rot} on the surface temperature for the NO/graphite system is shown in Fig. 3 for both the vibrational ground state (left) and the vibrational excited state (right). The solid lines correspond to complete accommodation of the rotational degree of freedom to the surface temperature. For the vibrational ground state of the unseeded molecules the experimental points follow this line up to a surface temperature of about 190 K, while at higher temperatures they deviate. At T_s higher than 350 K, T_{rot} approaches a

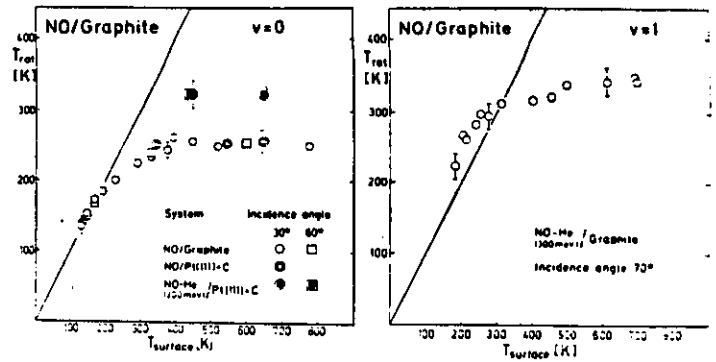

Fig. 3: Scattering of NO molecules from a pyrographite crystal and a carbon-covered Pt(111) surface. The rotational temperature is plotted versus the surface temperature for the vibrational ground state (left) and vibrationally excited molecules (right).

constant value of about 250 K. The results characterized by open symbols were obtained at an incoming energy of about 80 meV; increasing the average kinetic energy of the incoming NO molecules to about 200 meV (NO seeded in He) led to a somewhat higher rotational temperature (solid points).

Most of the rotational distributions were measured for NO molecules with an incidence angle of 30°. In this case, molecules predominantly in the specular direction were analyzed. Nearly the same rotational temperatures were obtained at a second incidence angle of 60°, where mainly molecules in the surface normal direction were investigated. Because of the bad angular resolution of this measurement a clear distinction between the fluorescence signal of diffusively and specularly scattered particles and, therefore, between their respective rotational temperatures was not possible. Later, however, we will see that the effective rotational temperature is slightly different for diffusively and quasi-specularly scattered molecules.

A similar dependence of T_{rot} on the surface temperature is measured for vibrationally excited NO molecules (Fig. 3, right). In this case, seeded NO molecules in v = 1 with a velocity of about 1400 m/s (~ 300 meV) impinged on the surface at an incidence angle of 70°. Only specularly scattered particles (scattering angle 64°) were analyzed. As with seeded molecules in the vibrational ground state, the rotational temperature approaches a constant value of about 335 K for high surface temperatures. For low surface temperatures our (preliminary) results show rotational temperatures higher than the corresponding surface temperatures, which could be a result of either the vibrational excitation or the high incoming translational energy. An evaluation

of vibrational ground state measurements with seeded NO molecules will clarify this effect. From these results we can conclude that the survivability of vibrational states is high, and that the rotational degree of freedom behaves independently of the vibrational excitation, which means a decoupling of rotation and vibration for the NO/graphite system.

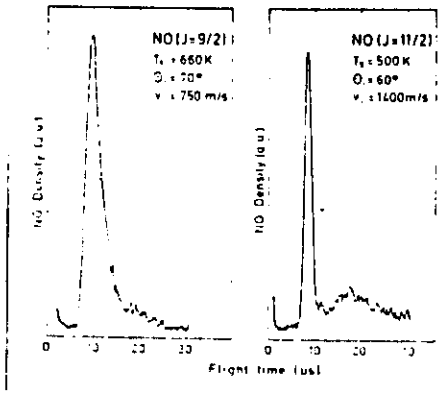

Fig. 4: Time-of-flight spectra of unseeded (left) and seeded (right) NO molecules scattered from a high temperature graphite surface in the specular direction.

For the measurement of state and angle resolved velocity distributions (in the vibrational ground state) the scattered molecules are ionized from a specific rotational state [6d]. Since the translational energy is conserved during photoionization, the time-of-flight spectra of the ions correspond directly to the velocity distributions of the parent neutral molecules. These time-of-flight measurements show that the spectra are nearly independent of the rotational states for all scattering angles. In the specular direction, they are composed of a very high quasi-specular peak of very fast molecules and a longer tail resulting from particles with lower velocities; see Fig. 4. In the left part, unseeded NO molecules with an incoming velocity v_i of 750 m/s were scattered from a high temperature graphite surface in the specular direction. The outgoing time-of-flight spectrum exhibits an overlapping of specularly (fast) and diffusively (slow) scattered molecules. For seeded incoming molecules, however, the flight time is shorter and the distribution has a smaller width. Therefore, specularly and diffusively scattered particles appear clearly separated as a result of their different arrival times at the ion multiplier (right side of Fig. 4).

Comparing the time of-flight spectra of molecules in different rotational states, we find the diffusive part to be stronger - relative to the specular part - for higher rotational states than for lower J-states. Consequently the diffusively scattered molecules gain more rotational energy during the scattering process than the specular ones. The diffusive and specular parts can be independently characterized by two rotational temperatures, with T_{rot} of the diffusively scattered molecules being about 20 % higher than that of the specularly scattered ones [6d].

Changing the position of the surface relative to the cage leads to velocity distributions of molecules with different scattering angles. Molecules scattered in the specular direction show a behaviour similar to Fig. 4, molecules scattered at a smaller angle and at low surface temperatures exhibit a velocity distribution with a smaller average velocity corresponding to the diffusive part of the angular distribution. This slow diffusive part disappears when the particles are scattered from a sufficiently hot surface. In this case, the scattered molecules show a clean lobular angular distribution where the peak velocity is dependent on both the incidence and the scattering angle. This is demonstrated in Fig. 5. Increasing the incidence angle leads to an increasing shift of the angular distribution maximum to lower scattering angles. Simultaneously, the average velocity in the direction of the angular maximum increases. However, the velocities inside a scattering lobe are not constant: they increase with decreasing scattering angle (Fig. 5, right).

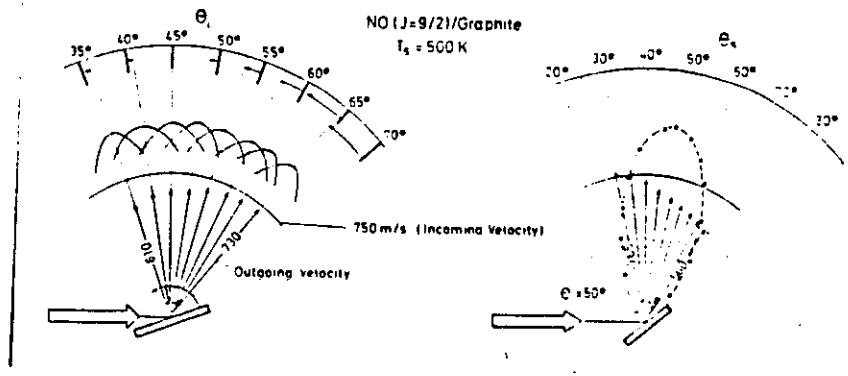

Fig. 5: Average velocity of scattered NO molecules (arrows) as a function of the incidence angle Θ_i (left) and the scattering angle Θ_s (right). The maximum of the scattering lobe is shifted to smaller scattering angles for $\Theta_i > 45°$ and to larger angles for $\Theta_i < 45°$ (left).

With inceasing surface temperature, the average velocity of the scattered particles increases. Figure 6 summarizes this effect as a function of the scattering angle for NO (J = 9/2) molecules with an incidence angle of 70°. It is also obvious that the variation of the velocities inside the scattering lobe increases with the surface temperature. These effects can be so substantial that some of the scattered molecules show a larger velocity

than the incoming ones, especially for high surface temperature, large incidence and small scattering angles.

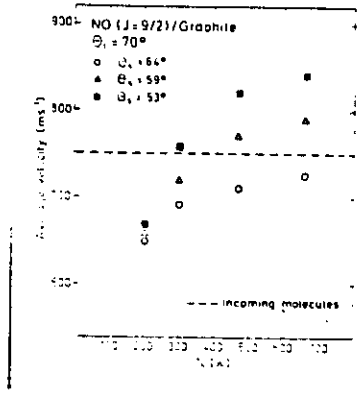

Fig. 6: Average velocity of scattered NO molecules versus surface temperature for different scattering angles.

DISCUSSION

Certainly the above results reflect the microscopic energy exchange processes that take place during different stages of the molecule surface interaction. Extensive numerical integration of the classical motion of the gas molecule and the nearby surface and bulk atoms using an empirical interaction potential for the scattering and desorption of NO molecules from Ag(111) and Pt(111) yielded satisfactory agreement with the experimental observations [16]. Such calculations, however, can only be performed for simple systems and even there the number of parameters to be adjusted in the assumed interaction potential is not to be minimized; furthermore only a few features of this potential seem to be relevant as the gas molecule interacts with a large number of surface and bulk atoms.

On the other hand it is well established that a relatively small number of the constituant atoms quite closely reproduces the properties of the infinite surface and bulk material and, in particular, the density of states for all degrees of freedom, electronic or ionic. Hence an approach that from the outset introduces the collective dynamical properties of the surface and the bulk should be appropriate and in practice very useful for a systematic study of different gas molecule/surface systems. From the fundamental point of view it is of course of considerable interest to extent the applicability of macroscopic solid state aspects down to a microscopic scale and study the accommodation between individual molecular motion and collective one. As it will be shown below transport properties can be used and account surprisingly well for the observed features. Combined with the extensive calculations [15] that use detailed molecular dynamics such an approach may provide a more unifying reformulation of the microscopic energy transfer processes.

From the previous observations one may assume that to a first approximation the translation, rotation and vibration of the molecule are decoupled and accordingly each motion obtains its own thermal equilibrium separately from the others, in particular because of the different energy spacings. We concentrate our attention on the rotational motion and we admit that the observed rotational temperature T_{rot} is reached during the separation stage of the gas molecule from the surface. We proceed to determine this T_{rot}.

During the short duration of the separation stage, of the order of a few femtoseconds, a nonequilibrium situation occurs and the thermodynamic equilibrium that is expected to exist between the surface and the bulk in the stationary regime is destroyed; this is due to the vastly different dynamical features of the collective surface and bulk motions respectively [17]. The gas molecule together with the nearby surface maintains during this stage a local equilibrium at a temperature T_{rot} which is different from the bulk temperature T_B; the latter will be taken as the reservoir. The resulting nonequilibrium is restored through heat conduction from the bulk to the molecule complex which during the interaction undergoes energy redistribution and relaxation. Let us admit that this can be described by a rate equation for the rotational energy

$$dE_{rot}/dt = - E_{rot}/\tau + j_T \qquad (1)$$

where τ is a relaxation or memory time of the rotational energy redistribution; j_T is the thermal energy per unit time transmitted accross the effective cross section of the molecule S which depends on its orientation on the surface; let us put $S = d^2$ where d is a characteristic molecular dimension projected on the surface. We set

$$j_T = - \kappa S(T_{rot} - T_B)/a \qquad (2)$$

where κ is the thermal conductivity [18,19] at the bulk temperature T_B and a is a characteristic surface depth. At local equilibrium $dE_{rot}/dt = 0$ and $E_{rot} = kT_{rot}$ for a linear molecule so that

$$T_{rot} = \tau d^2\kappa(T_B - T_{rot})/ka = \alpha(T_B - T_{rot}) \qquad (3)$$

or

$$T_{rot} = T_B\alpha/(1 + \alpha). \qquad (4)$$

The main temperature dependence in α comes through κ, the latter behaves quite differently for metals and dielectrics, respectively.

For crystalline dielectrics phonons are responsible [18] for heat conduction and for $T_B \gtrsim \Theta_D$, the Debye temperature [18], $\kappa \sim 1/T_B^{1+\varepsilon}$ where roughly $0 < \varepsilon < 1$; for an ideal crystalline dielectric $\varepsilon = 0$. For metals the electrons are mainly responsible for heat conduction and for $T_B \ll \Theta_F$, the Fermi temperature [18], $\kappa \sim 1/T_B^{1+\varepsilon}$ where now $-1 < \varepsilon < 0$ and $\varepsilon = -1$ for an ideal Fermi metal; for $T_B \gg \Theta_D$ or impure metals or disordered alloys the heat conduction becomes again dominated by phonons.

From these considerations on κ one may write in general $\alpha = \Lambda/T_B^{1+\varepsilon}$ with $-1 \leq \varepsilon \leq 1$ or

$$T_{rot} = T_B/(1 + T_B^{1+\varepsilon}/\Lambda) \qquad (5)$$

which accounts for the observed behaviour of T_{rot} as a function of T_B in all studied cases with $-1 < \varepsilon < 0$ for metals and $0 < \varepsilon < 1$ for crystalline dielectrics or dielectric layers on metals. It is instructive to have an order of magnitude estimation. Thus for the scattering of a NO molecule from an ideal dielectric ($\varepsilon = 0$) like NaCl where $\kappa = \chi/T_B$ with $\chi \cong 40$ J cm^{-1}s^{-1}, $a \cong 10$ Å, $d \cong 2 \cdot 10^{-8}$cm and $\tau \cong 3 \cdot 10^{-14}$s we obtain $\Lambda = T_{sat} \cong 300$ K and (5) can be written

$$T_{rot} = T_B / (1 + T_B/T_{sat}) \qquad (6)$$

where T_{sat} is a saturation temperature for the rotational energy distribution. In contrast for an ideal metal $\varepsilon = -1$ and one obtains a straight line with a slope $\Lambda/(1 + \Lambda)$ from eq. (4).

The above considerations are valid for $T_B > \Theta_D$ where almost all phonons are available for thermal conduction. For $T_B \ll \Theta_D$ (Debye regime) the number of phonons available for conduction is more restricted and $\kappa \sim (T_B/\Theta_D)^3$ and according to (3) T_{rot} may even be larger than T_B for dielectrics in the Debye regime; as $\Theta_D \cong 100$ - 200 K for most cases this situation should occur below 30 - 50 K; in this regime, however, quantum effects may become partially important.

The above model should apply both for desorption as well as for scattering since T_{rot} is essentially determined during the separation stage which has a very short memory. In the short times involved in the scattering interaction, however, partial coupling with translation or vibration mediated through the surface may occur. Such a situation can be accounted for by additional energy flows in (1). Thus coupling to translational motion to a first approximation leads again to T_{rot} described by (6) with a slightly larger T_{sat} in the case of an ideal dielectric and a slope > 1 for $T_B < T_{sat}$.

The use of this model for the rotational motion can be justified on account of the small rotational energy spacing of all molecules heavier than deuterium. Expressed in a temperature scale this spacing is Θ_{rot} and is smaller than 3 K so that classical heat transport is valid. The situation is expected to be quite different in the case of vibrational motion where the energy spacing corresponds to a temperature $\Theta_{vib} \cong 2700$ K which is a huge energy amount unlikely to be transferred rapidly; molecules vibrationally excited in the bulk are expected to lose at most ~ 300 K per ps [20] and thus a very long time with respect to the duration of the separation stage is required to channel out the energy $k\Theta_{vib}$ unless resonant quantum transfer effects with the phonons or other collective modes are present. Thus a vibrationally excited molecule in many respects can be expected to show the same behaviour as in its ground vibrational state in particular as far as the rotational temperature is concerned.

In conclusion within the stated assumptions and approximations the above model provides a remarkably straightforward explanation of the observed behaviour and relates it to macroscopic parameters. Extensive application to a large number of cases should allow one to better define its range of applicability and establish its link with the models based on detailed molecular trajectory dynamics.

ACKNOWLEDGEMENT

One of the authors (C.F.) sincerely thanks the Alexander von Humboldt Foundation for a senior Humboldt award.

References

1. C.R. Brundle and H. Morawitz, Vibrations at Surfaces (Elsevier, Amsterdam, 1983).
2. H. Ibach and D.L. Mills, Electron Energy Loss Spectroscopy and Surface Vibrations (Academic, New York, 1982).
3. R.J. Madix and J. Benziger, Annu. Rev. Phys. Chem. 29, 285 (1978).
4. M.J. Cardillo, Annu. Rev. Phys. Chem. 32, 331 (1981).
5. C.W. Muhlhausen, J.A. Serri, J.C. Tully, G.E. Becker, M.J. Cardillo, Isr. J. Chem. 22, 315 (1982).
6. (a) F. Frenkel, J. Häger, W. Krieger, H. Walther, C.T. Campbell, G. Ertl, H. Kuipers, J. Segner, Phys. Rev. Lett. 46, 152 (1981);

(b) F. Frenkel, J. Häger, W. Krieger, H. Walther, G. Ertl, J. Segner, W. Vielhaber, Chem. Phys. Lett. 90, 225 (1982); (c) J. Segner, H. Robota, W. Vielhaber, G. Ertl, F. Frenkel, J. Häger, W. Krieger, H. Walther, Surf. Sci. 131, 273 (1983); (d) J. Häger, Y.R. Shen, H. Walther, Phys. Rev. A 31, 1962 (1985); (e) J. Häger and H. Walther, J. Vac. Sci. Technol. B 3, 1490 (1985).

7. (a) A.W. Kleyn, A.C. Luntz, D.J. Auerbach, Phys. Rev. Lett. 47, 1169 (1981); (b) A.W. Kleyn, A.C. Luntz, D.J. Auerbach, Surf. Sci. 117, 33 (1982); (c) A.C. Luntz, A.W. Kleyn, D.J. Auerbach, Phys. Rev. B 25, 4273 (1982); (d) J.E. Hurst, L. Wharton, K.C. Janda, D.J. Auerbach, J. Chem. Phys. 78, 1559 (1983); (e) C.T. Rettner, F. Fabre, J. Kimman, D.J. Auerbach, Phys. Rev. Lett. 55, 1904 (1985).

8. (a) G.M. McClelland, G.D. Kubiak, H.G. Rennagel, R.N. Zare, Phys. Rev. Lett. 46, 831 (1981); (b) G.D. Kubiak, J.E. Hurst, Jr., H.G. Rennagel, G.M. McClelland, R.N. Zare, J. Chem. Phys. 79, 5163 (1983).

9. (a) M. Asscher, W.L. Guthrie, T.H. Lin, G.A. Somorjai, Phys. Rev. Lett. 49, 76 (1982); (b) M. Asscher, W.L. Guthrie, T.H. Lin, G.A. Somorjai, J. Chem. Phys. 78, 6992 (1983); (c) W.L. Guthrie, T.H. Lin, S.T. Cever, G.A. Somorjai, J. Chem. Phys. 76, 6398 (1982).

10. (a) H. Zacharias, M.M.T. Loy, P.A. Roland, Phys. Rev. Lett. 49, 1793 (1982); (b) J. Misewich, H. Zacharias, M.M.T. Loy, Phys. Rev. Lett. 55, 1919 (1985).

11. J.S. Hayden and G.J. Diebold, J. Chem. Phys. 77, 4767 (1982).

12. (a) J.W. Hepburn, F.J. Northrup, G.L. Ogram, J.C. Polanyi, J.H. Williamson, Chem. Phys. Lett. 85, 127 (1982); (b) D. Ettinger, K. Honma, M. Keil, and J.C. Polanyi, Chem. Phys. Lett. 87, 413 (1981).

13. J.B. Cross and J.B. Lurie, Chem. Phys. Lett. 100, 174 (1983).

14. (a) D.A. Mantell, S.B. Ryali, G.L. Haller, J.B. Fenn, J. Chem. Phys. 78, 4250 (1983); (b) D.A. Mantell, Y.F. Maa, S.B. Ryaly, G.L. Haller, J.B. Fenn, J. Chem. Phys. 78, 6338 (1983).

15. R.R. Lucchese and J.C. Tully, J. Chem. Phys. 80, 3451 (1984).

16. C.W. Muhlhausen, L.R. Williams, J.C. Tully, J. Chem. Phys. 83, 2594 (1985).

17. R.F. Wallis, Progr. Surf. Sci. 4, Ed. S.G. Davinson, 233, (1973)

18. N.W. Ashcroft and N.D. Mermin, Solid State Physics, (Holt-Saunders, Tokio, 1981), chp. 25.

19. C. Kittel, Introduction to Solid State Physics, (John Wiley, N.Y., 1976), chps. 5 and 6.

20. A. Seilmeier and W. Kaiser, (private communication)